Available online at www.sciencedirect.com
ScienceDirect
Journal of the European Ceramic Society 29 (2009) 473–480
www.elsevier.com/locate/jeurceramsoc

Processing of silicon carbide–boron carbide–aluminium composites

Gursoy Arslan *, Ayse Kalemtas

Anadolu University, Department of Materials Science and Engineering, Iki Eylul Campus, 26480 Eskisehir, Turkey

Received 9 February 2008; received in revised form 30 May 2008; accepted 6 June 2008
Available online 23 July 2008

Abstract

The aim of this work was to shed light on the wetting mechanism in the SiC–B_4C–Al system and to explore processing routes that enable infiltration of Al alloys into these ceramic powder mixtures without the formation of the deleterious reaction product Al_4C_3. For this purpose, powder mixtures consisting of SiC and pre-treated B_4C were pressureless infiltrated with Al alloys at relatively low temperatures under an inert gas atmosphere. Depending on the characteristics of the starting powders fully infiltrated composites were achieved in the temperature range of 935–1420 °C. It was observed that addition of pre-treated B_4C to SiC enabled complete infiltration of the ~0.6 cm thick preforms. The bulk density of all produced composites was >98% of the X-ray density. By controlling the surface chemistry and particle size of the starting powders as well as the processing conditions, the wetting behaviour and reaction kinetics of this system could be tailored so as to render fully dense SiC–B_4C–Al composites devoid of Al_4C_3.

Keywords: Composites; Carbides; SiC; Armour; Infiltration

1. Introduction

Wettability can be defined as the ability of a liquid to spread on a solid surface, and it represents the extent of intimate contact between a liquid and a solid.[1] Unfortunately, the wettability of ceramic particles with liquid Al alloys is generally poor.[2]

Lack of wetting is usually attributed to the presence of contamination, moisture, or a gas layer that covers the ceramic particle surface, to the Al_2O_3 layer that covers liquid Al and/or to the native SiO_2 layer that ordinarily covers SiC particles. In all these cases the molten metal matrix is hindered from coming into contact with the surface of the individual particles.[3–7]

Various procedures have been recommended to improve the wetting of ceramic particles by liquid metal, and include: (i) increasing metal liquid temperature,[8] (ii) the addition of some surface-active/reactive elements such as Mg, Li, Ca, Ti, or Zr into the matrix alloy,[9–13] (iii) coating or oxidising the ceramic particles,[14–18] and (iv) cleaning the particles, for example by preheat treatment.[19–21] The principle methods to improve wetting are based on (1) increasing the surface energy of the solid, (2) decreasing the surface tension of the liquid alloy, or (3) decreasing the solid–liquid interfacial energy, at the particle–matrix interface.[22,23]

Two of the major problems frequently encountered in the processing by the pressureless infiltration method are (i) the presence of considerable levels of residual porosity and (ii) the development of unwanted reaction products (Al_4C_3, Al_4SiC_4).[24]

Residual porosity is related to an inadequate wetting of SiC by molten Al and unwanted reactions/phases developed from the dissolution of the SiC reinforcement by the liquid Al.[25–27] At temperatures above the melting point of Al, and under atmospheric pressure, SiC becomes thermodynamically unstable; interfacial reactions may occur and result in reaction products such as Al_4C_3[25,27–34] and Al_4SiC_4.[35–37] Because the solubility of C in liquid Al is very low, the threshold C activity values for Al_4C_3 formation are small. The C atoms that go into solution will react almost immediately with Al to form Al_4C_3 either as a continuous layer or as discrete precipitates around the SiC particles.[38] Not only does this reaction cause the dissolution/degradation of the SiC reinforcing particles and result in weakening of the composite, but also both Al_4C_3 and Al_4SiC_4 are thermodynamically unstable and have

* Corresponding author. Tel.: +90 222 3213550x6361; fax: +90 222 3239501.
E-mail address: garslan@anadolu.edu.tr (G. Arslan).

0955-2219/$ – see front matter © 2008 Elsevier Ltd. All rights reserved.
doi:10.1016/j.jeurceramsoc.2008.06.007

a tendency to hydrolyse slowly with the atmospheric moisture to form Al-hydroxide thereby enhancing crack propagation in the composite by the moisture-induced corrosion of the Al_4C_3 phase.[35,38,39]

2. Aim of the current study

B_4C–Al composites are potential candidate materials to be used, for example, in impact applications. Although novel processing routes such as pressureless melt infiltration already have ensured fabrication of these composites at low processing costs, the relatively high cost of B_4C powder limits their widespread usage.

SiC, on the other hand is being produced in larger scales and it also has a wider field of application areas when compared with B_4C. The price of SiC powder, accordingly, is lower than that of B_4C while its ballistic performance is close to that of B_4C.

Therefore, the main driving force to conduct this work was to produce SiC–B_4C–Al composites with as low a B_4C content as is possible that may be used for impact applications and explore processing routes that preserve the cost-effectiveness of the pressureless melt infiltration method.

Another important goal of this study was to show that B_4C addition provides an alternative, effective and simple approach to improve the wettability of SiC by Al. That is why the starting SiC powders were not coated or oxidized prior to the infiltration process and a Si-deficient alloy with a relatively low Mg content was used as a source of Al.

3. Experimental

The SEM micrographs of the starting powders are shown in (Fig. 1).

Passivation of starting B_4C powders was achieved by heat-treating them in the absence of free carbon at 1370 °C for 2 h under an Ar gas atmosphere prior to the infiltration process.[40]

SiC and B_4C powders were planetary ball milled in alcohol media. After milling, the slurry was dried in a rotary evaporator.

Preforms were prepared by uniaxially pressing the SiC–B_4C powder mixtures at 100 MPa. Polyethylene glycol (PEG) was used as a binder.

SiC–B_4C–Al composites were produced by melt infiltrating 7075 Al alloy blocks into porous SiC–B_4C preforms under an Ar gas atmosphere. Infiltration temperatures were chosen between 935 and 1420 °C. Heating rate applied was 5 °C/min up to 900 °C and 10 °C/min onwards up to the infiltration temperature. Cooling rate from the infiltration temperature to 900 °C was 10 °C/min and then 5 °C/min down to room temperature.

X-ray diffraction (Rigaku Rint 2200, Tokyo, Japan) was performed using monochromatic Cu-Kα radiation (λ = 1.5406 Å).

Microstructural studies of the composites were performed with scanning electron microscopes (ZEISS EVO 50 EP and ZEISS SUPRA 50 VP, Germany) both attached with an energy dispersive X-ray spectrometer (Bruker AXS XFlash, Germany and Oxford Instruments Inca Energy model 7430, England, respectively).

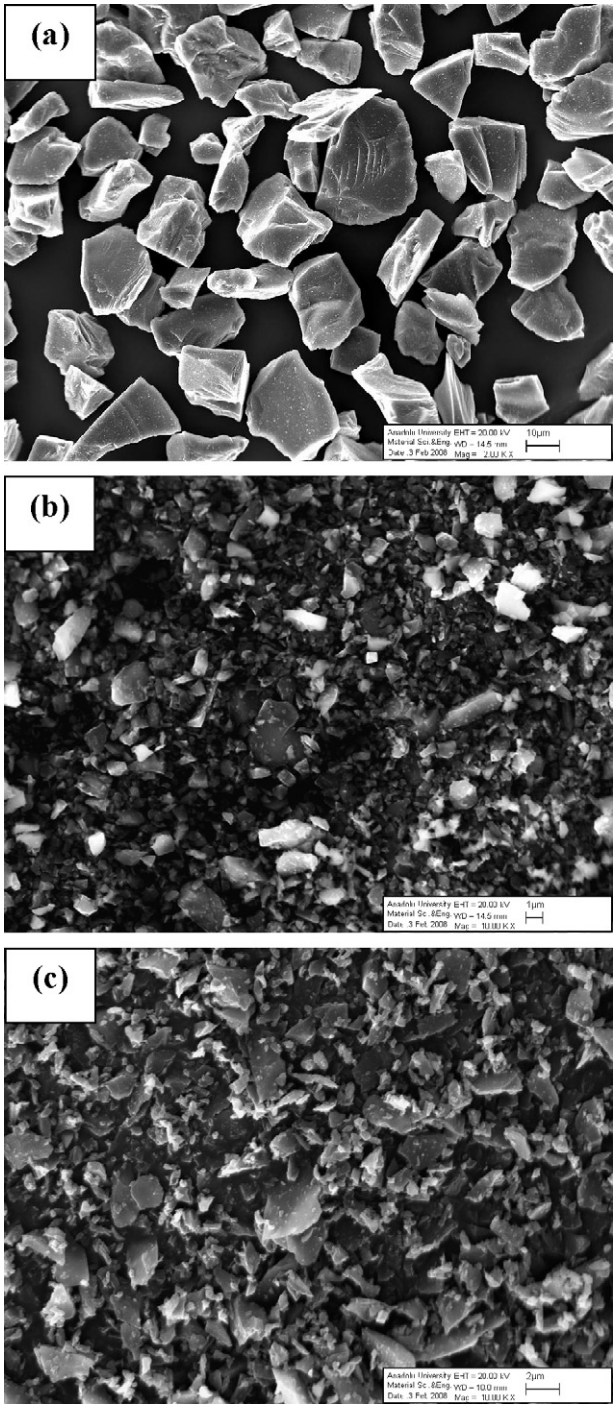

Fig. 1. SEM micrographs of starting powders. (a) coarse SiC, (b) fine SiC and (c) fine B_4C.

4. Results

The lowest infiltration temperatures and infiltration times of the prepared compositions to result in full infiltration of the ~6 mm high pellets are given in Table 1. Among the produced composites 80S20B has the lowest infiltration temperature of 935 °C but at the expense of higher infiltration time. Similarly, the compositions 60S40B and 70S30B have the lowest infiltration times but at the expense of somewhat increased infiltration

Table 1
Chemical composition of prepared powder mixtures and limit conditions of infiltration

Composition	SiC (wt.%)	B_4C (wt.%)	Temperature (°C)	Time (min)
50S50B	50	50	985	60
60S40B	60	40	1035	10
70S30B	70	30	1035	10
80S20B	80	20	935	60
90S10B	90	10	985	30
95S5B	95	5	1130	60
100S[a]	100	0	1420[a]	60[a]

[a] Partial infiltration (~2.4 mm).

temperatures. Fig. 2 depicts the variation of the open porosity content and lowest infiltration temperature as a function of B_4C content. It indicates that there is a strong relationship between the amount of open porosity, infiltration temperature and B_4C content of the powder mixture. The amount of open porosity content is relatively low (<1.5 wt.%) in composites containing less than 10 wt.% B_4C, but as the B_4C content is reduced below this value it increases sharply reaching 2.76% at 5 wt.% B_4C. The variation of the lowest infiltration temperature with the B_4C content follows a similar trend. Full infiltration takes place at temperatures below 1050 °C in composites containing at least 10 wt.% B_4C, but as the B_4C content is further reduced it increases to 1130 °C at 5 wt.% B_4C. In the absence of B_4C, only partial infiltration (2.4 mm) was achieved at 1420 °C.

Variation of the green and bulk density of the composites as a function of B_4C content are shown in Fig. 3. It indicates that the green density of the searched compositions increases slightly with decreasing B_4C content reaching a maximum of 62.3% at the composition of 70S30B but then decreases with further reduction of added B_4C content. The lowest green density of ~52% was obtained in the compositions 95S5B and 100S. The bulk densities of the produced composites ranged in a relatively narrow band from 2.71 to 2.83 g/cm^3.

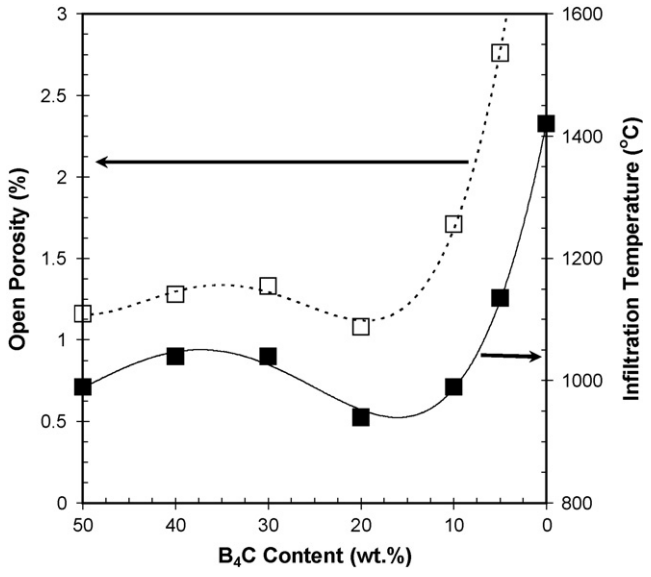

Fig. 2. Plot of open porosity content and lowest infiltration temperature of the produced composites as a function of B_4C content.

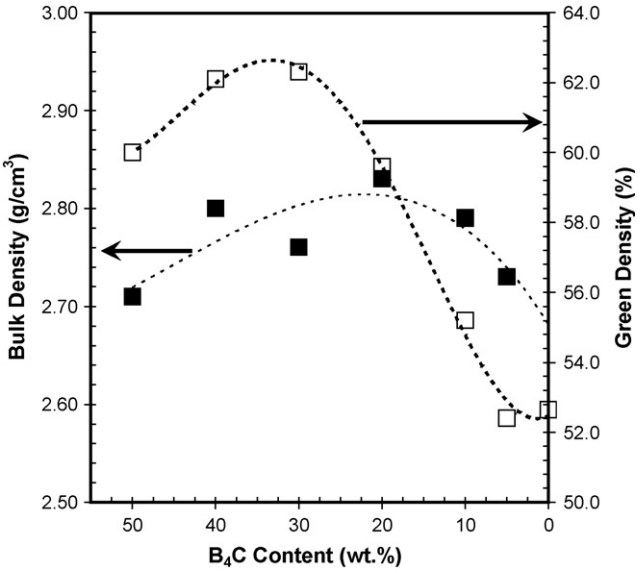

Fig. 3. Plot of green and bulk of the produced composites as a function of B_4C content.

Qualitative X-ray diffraction revealed that all produced composites contained the phases SiC, B_4C, Al, Al_3BC, and Si. Peaks belonging to the Al_4C_3 phase could not be proven to exist in the composites 80S20B (Fig. 4b), 60S40B, 50S50B, and 90S10B. Al_4C_3 formed in significant amounts in the composites 95S5B and 100S (Fig. 4c and d). XRD patterns of the composites 80S20B that were produced from coarse and fine SiC powders and infiltrated at the limiting conditions (935 °C/1 h)

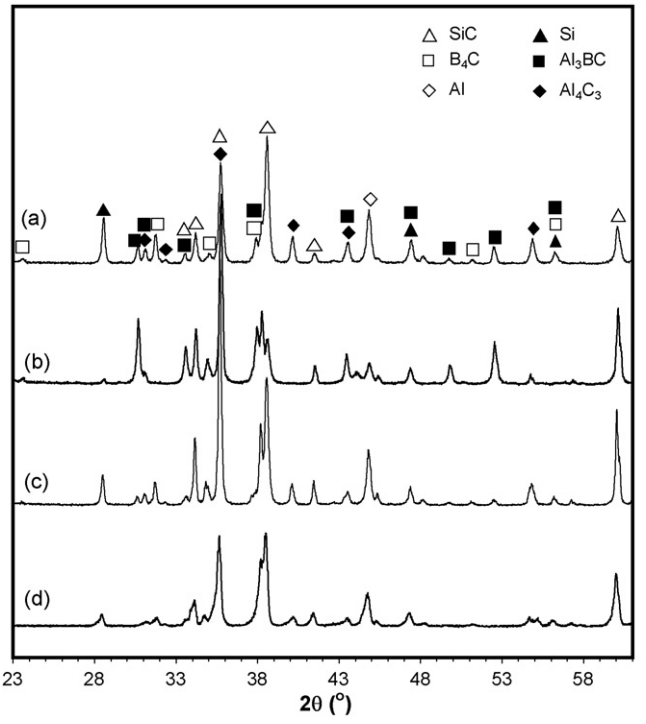

Fig. 4. XRD patterns of composites (a) 80fS20B (fine SiC powder) infiltrated at 935 °C for 1 h, (b) 80S20B infiltrated at 935 °C for 1 h, (c) 95S5B infiltrated at 1135 °C for 1 h and (d) 100S infiltrated at 1420 °C for 1 h.

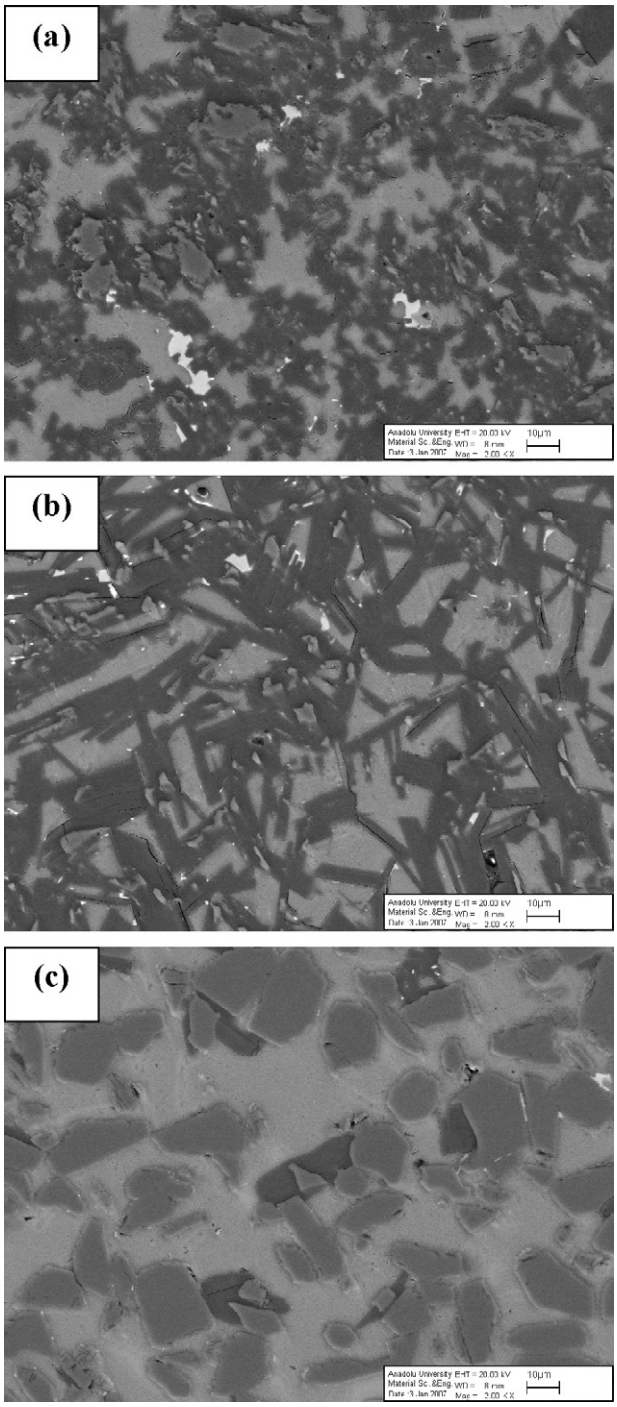

Fig. 5. SEM micrographs of the partially infiltrated composite 100S taken from (a) the top layer, (b) the intermediate layer, and (c) the bottom layer.

are compared in Fig. 4a and b. It is seen that Al_4C_3 formation was suppressed completely by incorporating coarse SiC starting powders.

5. Discussion

The results obtained indicate that the produced SiC–B_4C–Al composites can be categorized in two main groups: (i) the first group is comprised of composites that can be pressureless infiltrated under the employed testing conditions only when the temperature is well in excess of 1050 °C, and in which platelet-shaped Al_4C_3 formation takes place in significant amounts (95S5B), (ii) while the second group includes the composites that can be infiltrated at temperatures below 1050 °C and in which the existence of Al_4C_3 could not be verified by XRD (50S50B, 60S40B, 80S20B and 90S10B).

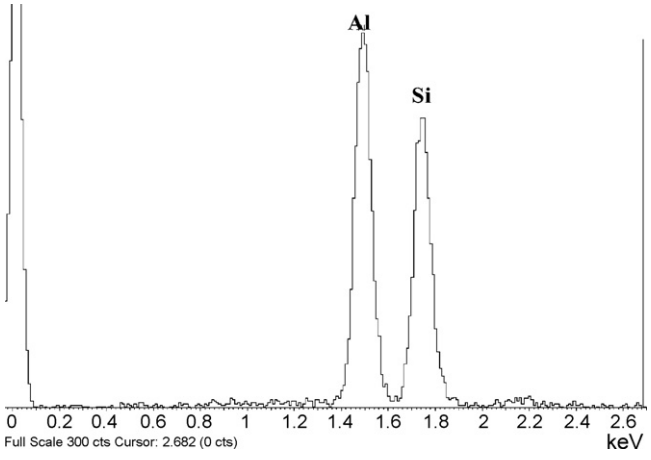

Fig. 6. EDX point analysis of the metallic matrix in the top layer of the partially infiltrated composite 100S.

The composites 100S, 95S5B and 80S20B were studied in detail to characterize their typical microstructural features. Based on these experimental findings an infiltration mechanism was proposed for the SiC–B_4C–Al system.

When the microstructure of the composite 100S is scanned from top to bottom three clearly distinguishable layers with different microstructural features becomes apparent (Fig. 5). These observations showed that there was high continuity at the Al/SiC interfaces with a low proportion of faults of contact or voids. Both observations are signs of a proper wettability between these two composite components.

The first layer (Fig. 5a) which is closest to the metal block-powder compact interface and is measured to have a thickness of about 700 μm, contains a small amount of undissolved SiC particles whose surfaces are irregularly shaped and dull. It is also seen that the average size of the coarse SiC particles has become smaller when compared with their initial size (Fig. 1a) due to extensive dissolution of them and the subsequent formation of dull-shaped and dark grey-coloured reaction products that dominantly surround these SiC particles. As verified by XRD results (Fig. 4d), the reaction product is Al_4C_3. XRD pattern of this composite and point analyses taken from the light grey phase indicate that the metal matrix is an Al–Si eutectic (Fig. 6). Since the Al alloy used did not contain any Si initially, it must have originated from the SiC phase. The low degree of interconnectivity of the Al–Si matrix suggests that the microstructure was about to be locked. In fact, there are regions where the Al–Si eutectic alloy has been completely isolated by Al_4C_3 particles with a globular morphology from the remaining metal matrix (Fig. 5a).

The intermediate layer (Fig. 5b) was measured to be about 650 μm thick. SiC particles that did not dissolve completely

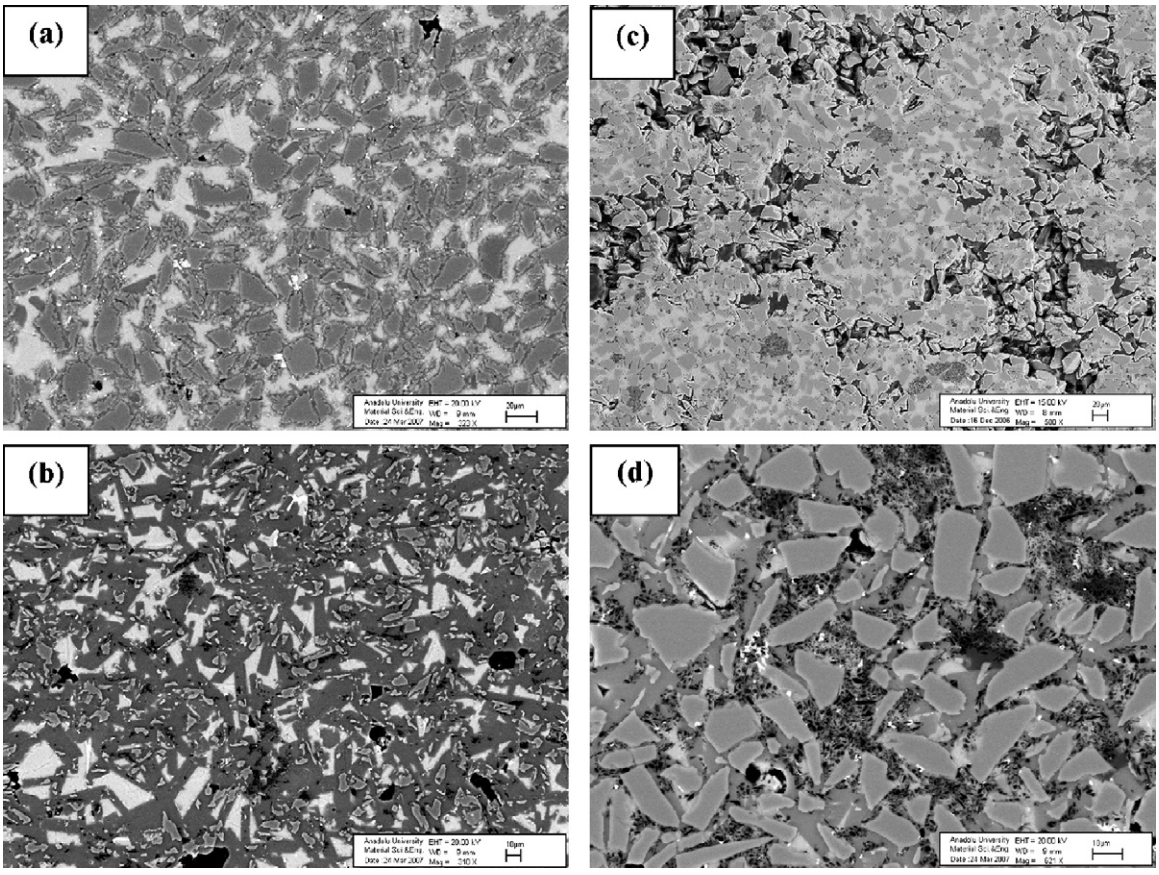

Fig. 7. SEM micrographs of the composite 95S5B taken from (a) the layer close to the preform/metal source interface (top layer), (b) the intermediate layer, (c) the layer distant to the interface (bottom layer), and (d) 80S20B (no layered cross-section).

were still observed but to a much less extent and of much smaller particle size indicating that there was more time for the SiC dissolution process to take place in this layer. The XRD pattern of this layer and point analysis taken from this phase confirmed the presence of Al_4C_3. This Al_4C_3, however, appears in the form of platelets with a relatively high aspect ratio. Because of the large amount of tiny Al_4C_3 platelets the interconnectivity of the metal matrix is completely lost, leaving many Al–Si islands isolated. This in turn infers that almost all channels through which the liquid alloy has to flow has been completely locked thereby preventing a continuous and easy supply of liquid metal to the lower parts of the composite. Comparison of (Fig. 5b and c) nicely depicts the narrowing of the channel width and locking of the microstructure in the intermediate layer. The SiC particles in contact with the liquid alloy thus had enough time to dissolve almost completely (Fig. 5b).

The third layer (Fig. 5c), which is closest to the unfiltrated powder compact had a thickness of about 1150 μm and was comprised of a large number of SiC particles with a morphology and size close to that of the starting SiC powders (Fig. 1). XRD results confirmed the absence of Al_4C_3 in this layer. In agreement with the reduced reactivity between SiC and Al in this layer and the absence of tiny platelet shaped Al_4C_3 particles, the degree of interconnectivity in the metallic phase was high.

Addition of as low as 5 wt.% B_4C to the SiC powder compact resulted in a drastic decrease in the infiltration temperature from 1420 to 1130 °C (Table 1). Furthermore, although the composition 100S could only be partially infiltrated, full infiltration was achieved in 95S5B. Addition of another 5 wt.% to the SiC–B_4C powder mixture caused a further noteworthy reduction in the infiltration temperature and time (Table 1). Further enrichment of the SiC–B_4C powder mixture in B_4C, however, was observed to influence the infiltration temperature to a less extent.

When the microstructure of 95S5B is scanned from top to bottom (Fig. 7a–c) the inhomogeneity in the distribution of pores, SiC particle shape and size, and phase composition becomes apparent. The top and intermediate layers are characterized by a relatively low porosity content, SiC particles having many intrusions and extrusions, Al_4C_3 particles formed, hardly observable B_4C particles and an Al–Si matrix (Fig. 7a and b). They exhibit a well-defined reaction zone between the SiC and the metal matrix with a contour that is dull and highly irregular. The reacted layers are continuous, completely surrounding the SiC particles. The presence of the reaction products Al_4C_3 and Si in these layers was confirmed by the results of the XRD analysis (Fig. 8b and d).

The bottom layer (Fig. 7c) is characterized by a relatively large porosity content, SiC particles maintaining their initial shape and size, lack of Al_4C_3 particles, and clusters of unreacted B_4C particles left in the space between the coarse SiC particles. No obvious reaction layer is apparent at the SiC–Al interface. This observation is in agreement with the results of X-

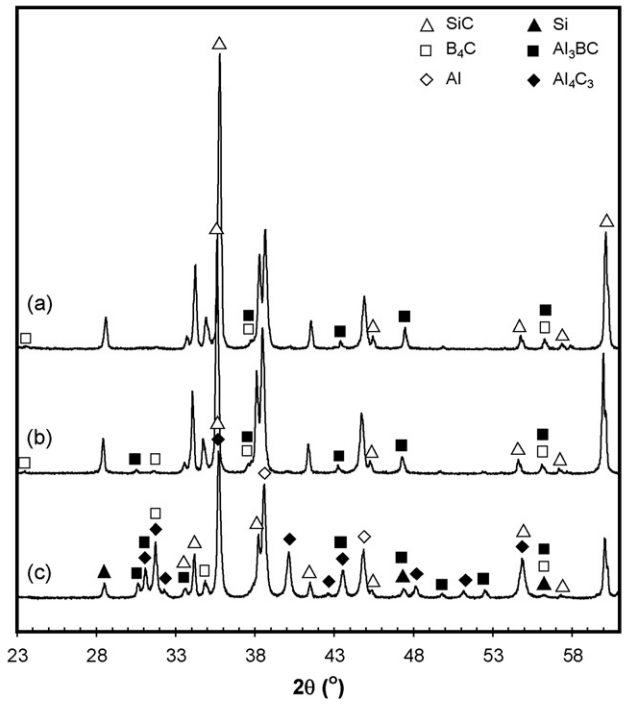

Fig. 8. XRD patterns of the composite 95S5B infiltrated at 1135 °C for 1 h. (a) bottom layer, (b) intermediate layer and (c) top layer.

ray diffraction analysis, which indicated that Al_4C_3 formation did not take place in this layer (Fig. 8a).

Scanning the microstructure of the composite 80S20B through its cross-section revealed that, unlike in 95S5B, there are no significant differences in microstructural features as one moves from top to bottom. Its microstructure is characterized by the absence of Al_4C_3 and a homogeneous distribution of fine B_4C particles in the space between the coarse SiC particles (Fig. 7d). The absence of Al_4C_3 was confirmed by XRD analysis (Fig. 4b). Comparison of the particle sizes of SiC and B_4C with their initial size (Fig. 1) illustrates that most of the B_4C particles have decreased in size while the SiC particles preserve their initial size. This indicates that dissolution of B_4C occurred preferentially, which may be attributed to its finer particle size. However, a higher dissolution rate of B_4C with respect to SiC was also observed by Chernyshova and Rebrov.[41] This in turn indicates that the reaction product Al_3BC predominantly results from the interaction between B_4C and Al, while that metallic Si, if observed, should be present in small amounts. This reasoning is in very good agreement with the XRD powder pattern of this composite which shows a very weak $Si_{1\,1\,1}$ peak at $2\theta \approx 28.44^\circ$ and a relatively strong $Al_3BC_{1\,0\,1}$ peak at $2\theta \approx 30.56^\circ$, (Fig. 4b).

Based on these experimental findings the following infiltration mechanism is proposed. Once a true Al–B_4C interface is created interaction proceeds by the classical dissolution–precipitation mechanism (Fig. 9a). C and B atoms migrate by liquid-phase diffusion from the surface of B_4C where Al supersaturates in C and B (dissolution) to faces of Al_3BC crystals that are growing from the metal (precipitation). As maximum solubility of these elements in Al are very low, simple dissolution process ends very quickly. It is followed by nucleation and growth of mainly Al_3BC crystals from an Al matrix supersaturated in B and C (Fig. 9b).[42] In places where Al_3BC crystals are fixed and begin to grow, coarse SiC particles surrounded by Al_3BC particles are protected against further attack; while in places where liquid Al remains in direct contact with the surface of SiC, dissolution continues. This is no longer true when growing Al_3BC crystals tend to join together and form a dense layer at the SiC surface (Fig. 9c). Further growth of reaction products obeys another mechanism that implies solid-state diffusion of B, C, or Al atoms through the growing Al_3BC layer.[42]

It was observed that Al_4C_3 did not form in the composites that contained B_4C contents equal to or greater than 10 wt.% in their starting powder mixtures. Therefore it is argued that 10 wt.% fine B_4C was enough to effectively cover the surfaces of coarse SiC particles with B_4C and hence Al_3BC. The consequence of this encapsulation is to restrict a direct contact between SiC and liquid Al and to form a solid barrier for the diffusion of Si and C atoms originating from the SiC particles. Apart from that, the formation of significant amounts of the Al-rich Al_3BC phase, especially in the vicinity of the SiC–Al interface depletes these regions in C and especially Al making the formation of Al_4C_3 even more difficult. Since Al_3BC does not have a needle- or plate-like morphology, the pore channels, through which the liquid alloy flows, although getting narrower, are not blocked completely.

Based on a previous work by Arslan et al.[43] it is reached that Al_3BC is the 3D compound enabling reactive wetting in the SiC–B_4C–Al system. Thus, the infiltration front may continue to penetrate deeper into the porous powder compact as long as Al continues to react with freshly exposed B_4C particles forming Al_3BC at the B_4C–Al interface, and the infiltration rate is faster than the reaction rate at the B_4C–Al interface.

It is proposed that there are two possible mechanisms for Al_3BC to improve the wettability in the SiC–B_4C–Al system. On the one hand, the reaction product Al_3BC might be more wettable by Al than is B_4C. On the other, the Al_3BC–Al system itself, like the B_4C–Al system, might have a non-wetting character. In the latter case, the improved wettability has to be attributed to a proper balance of interfacial energies at the (B_4C–Al_3BC)–Al interface.[44]

The formation of Al_4C_3 and Si in the SiC–Al system results in an expansion in volume of about 9.8% (densities of SiC, Al, Al_4C_3 and Si were taken as 3.22, 2.70, 2.99 and 2.33 g/cm^3, respectively) contributing to the narrowing of the pore channels.

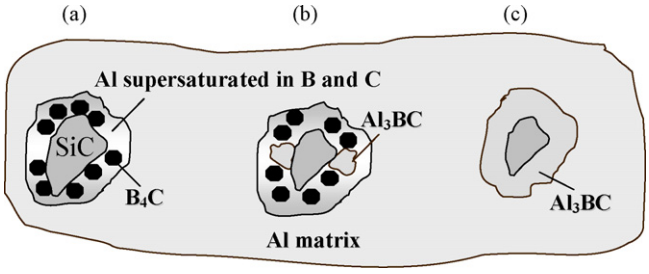

Fig. 9. Proposed infiltration model for the SiC–B_4C–Al system.

Al_4C_3 crystals precipitate out as elongated grains, which divide the originally large channels (Fig. 5c) between the SiC particles into many tiny channels (Fig. 5b), thus appreciably slowing down the infiltration rate. This significant reduction in the infiltration rate may lead to a switch in the infiltration mode from the reaction-controlled one to the infiltration-controlled one in the absence of sufficient B_4C and therefore Al_3BC.[45]

6. Conclusions

Compositions containing no B_4C could be infiltrated only partially and at relatively high infiltration temperatures (1420 °C).

Addition of fine B_4C to the powder mixture resulted in a drastic decrease in the infiltration temperature and fully infiltrated composites.

Composites having less than 10 wt.% B_4C had to be infiltrated at temperatures well in excess of 1050 °C. They were characterised to have a relatively high (>1.5 wt.%) porosity content, a layered microstructure across the specimen thickness, suffer from extensive dissolution of SiC particles and contained significant amounts of Al_4C_3.

Composites having at least 10 wt.% B_4C could be infiltrated at temperatures below 1050 °C. They were observed to have less than 1.5 wt.% open porosity, a homogeneous microstructure, and hardly contained Al_4C_3. Such composites were characterised to form a protective Al_3BC layer around the coarse SiC particles effectively suppressing the dissolution rate of them.

The reaction of SiC with Al to produce Al_4C_3 and metallic Si is accompanied by a volume expansion in the order of 10%. This, coupled with the plate-like morphology of Al_4C_3 crystals divides the originally large channels into many tiny channels thus blocking the flow of liquid metal and significantly reduces the infiltration rate.

Acknowledgements

We are grateful to The Foundation for Scientific Research Projects of Anadolu University for funding the present study (Project No. 030235). We also would like to acknowledge Research Assistant Erhan Ayas and Prof. Dr. Servet Turan for having conducted part of the SEM work.

References

1. Hashim, J., Looney, L. and Hashmi, M. S. J., The atomic arrangement in glass. *J. Mater. Process. Technol.*, 2001, **119**, 324–328.
2. Hashim, J., Looney, L. and Hashmi, M. S. J., The atomic arrangement in glass. *J. Mater. Process. Technol.*, 2001, **119**, 329–335.
3. Ray, S., Casting of composite components. In *Proceedings of the 1995 Conference on Inorganic Matrix Composites*, 1996, pp. 69–89.
4. Zhou, W. and Xu, Z. M., Casting of SiC reinforced metal matrix composites. *J. Mater. Process. Technol.*, 1997, **63**, 358–363.
5. Warren, R. and Anderson, C. H., Silicon carbide fibres and their potential for use in composite materials. *Composites*, 1984, **15**, 101–111.
6. Eustathopoulos, N., Joud, J. C., Desre, P. and Hicter, J. M., The wetting of carbon by aluminium and aluminium alloys. *J. Mater. Sci.*, 1974, **9**, 1233–1242.
7. Ribes, H., Dasilva, R., Suery, M. and Bretau, T., Effect of interfacial oxide layer in aluminium–silicon carbide particle composites on bond strength and mechanical behavior. *Mater. Sci. Technol.*, 1990, **6**, 621–628.
8. Levi, C. G., Abbaschian, G. J. and Mehrabian, R., Interface interactions during fabrication of aluminum alloy–alumina fiber composites. *Metall. Trans. A*, 1978, **9**, 697–711.
9. Dellanney, F., Rozen, L. and Deryterre, A., The wetting of solids by molten metals and its relation to the preparation of metal–matrix composites. *J. Mater. Sci. Lett.*, 1987, **22**, 1–16.
10. Champion, A. R., Krueger, W. H., Hartman, H. S. and Dhingra, A. K., In *Proceedings of the ICCM-2*. AIME, 1978, p. 883.
11. Hunt, W. H., In *Proceedings of the Conference on Interfaces in MMCs*. TMS-AIME, New Orleans, 1986, pp. 3–25.
12. Kimura, Y., Compatibility between carbon fiber and binary aluminum alloys. *J. Mater. Sci.*, 1984, **19**, 3107–3114.
13. Ray, S., M. Tech. Dissertation, IIT, Kanpur, India, 1969.
14. Kulkarni, A. G., Pai, B. C. and Balasubramanian, N., The cementation technique for coating carbon fibres. *J. Mater. Sci.*, 1979, **14**, 592–598.
15. Pai, B. C. and Rohatgi, P. K., Copper coating on graphite particles. *Mater. Sci. Eng.*, 1975, **21**, 161–167.
16. Rocher, J. P., Girot, F., Quinisset, J. M. and Naslain, R., In *Proceedings of the ECCM-1*, 1985, p. 634.
17. Abdul-Lattef, N. I., Ismael, K. A. R. and Goel, G. K., Preparation of Al–Al_2O_3–MgO cast particulate composites using MgO coating technique. *J. Mater. Sci. Lett.*, 1985, **4**, 385–388.
18. Rocher, J. P., Quinisset, J. M. and Naslain, A new casting process for carbon (or SiC-based) fibre-aluminium matrix low-cost composite materials. *J. Mater. Sci. Lett.*, 1985, **4**, 1527–1529.
19. Banerjee, A., Rohatgi, P. K. and Reif, W., *Metallurgy*, 1984, **38**, 656.
20. Rohatgi, P. K., Asthana, R. and Das, S., Solidification, structures, and properties of cast metal–ceramic particle composites. *Int. Met. Rev.*, 1986, **31**, 115–139.
21. Krishnan, B. P., Surappa, M. K. and Rohatgi, P. K., UPAL process: a direct method for producing cast aluminum alloy graphite composites. *J. Mater. Sci.*, 1981, **16**, 1209–1216.
22. Pai, B. C., Satyaranayana, K. G. and Robi, P. S., Effect of chemical and ultrasound treatment on the tensile properties of carbon fibres. *J. Mater. Sci. Lett.*, 1992, **11**, 779–781.
23. Tracey, M. H., *Mater. Sci. Technol.*, 1986, **4**, 227–230.
24. Aguilar-Martinez, J. A., Pech-Canul, M. I., Rodriguez-Reyez, M. and De La Pena, J. L., Effect of processing parameters on the degree of infiltration of SiC_p preforms by Al–Si–Mg alloys. *Mater. Lett.*, 2003, **57**, 4332–4335.
25. Iseki, T., Kameda, T. and Maruyama, T., Interfacial reactions between SiC and Al during joining. *J. Mater. Sci.*, 1984, **19**, 1692–1698.
26. Laurent, V., Chatain, D. and Eustathopoulos, N., Wettability of SiC by Al and Al–Si alloys. *J. Mater. Sci.*, 1987, **22**, 244–250.
27. Lloyd, D. J., Lagage, H., McLeod, A. and Morris, P. L., Microstructural aspects of Al–SiC particulate composites produced by a casting method. *Mater. Sci. Eng.*, 1989, **A107**, 73–80.
28. Viala, J. C., Bosselet, F., Laurent, V. and Lepetitcorps, Y., Mechanism and kinetics of the chemical interaction between liquid aluminium and silicon-carbide single crystals. *J. Mater. Sci.*, 1993, **28**, 5301–5312.
29. Lloyd, D. J., The solidification microstructure of particulate reinforced aluminium/SiC composites. *Comp. Sci. Technol.*, 1989, **35**, 159–179.
30. Lloyd, D. J. and Jin, I., A method of assessing reactivity between silicon carbide and molten Al. *Metall. Trans.*, 1988, **19A**, 3107–3109.
31. Warren, R. and Andersson, C. H., Silicon carbide fibres and their potential for use in composite materials. *Composites*, 1984, **15**, 101–111.
32. Lloyd, D. J., Particulate reinforced aluminium and magnesium matrix composites. *Int. Mater. Rev.*, 1994, **39**, 1–23.
33. Lee, J. C., Byun, J. Y., Oh, C. S., Seolc, H. K. and Lee, H. I., Effects of various processing methods on the interfacial reactions in SiCp/2024 Al composites. *Acta Mater.*, 1997, **45**, 5303–5315.
34. Park, J. K. and Lucas, J. P., Moisture effect on SiC_p/6061 Al MMC: dissolution of interfacial Al_4C_3. *Scripta Mater.*, 1997, **37**, 511–516.
35. Viala, J. C., Fortier, P. and Bouix, J., Stable and metastable phase equilibria in the chemical interaction between aluminium and silicon carbide. *J. Mater. Sci.*, 1990, **25**, 1842–1850.

36. Oh, S.-Y., Cornie, J. A. and Russel, K. C., Wetting of ceramic particulates with liquid aluminium alloys. Part I. Experimental techniques. *Metall. Trans. A*, 1989, **20**, 527–532.
37. Oh, S.-Y., Cornie, J. A. and Russel, K. C., Wetting of ceramic particulates with liquid aluminium alloys. Part II. Study of wettability. *Metall. Trans. A*, 1989, **20**, 533–541.
38. Tham, L. M., Gupta, M. and Cheng, L., Effect of limited matrix-reinforcement interfacial reaction on enhancing the mechanical properties of aluminium–silicon carbide composites. *Acta Mater.*, 2001, **49**, 3243–3253.
39. Kosolapova, T. Y., *Carbides Properties, Production and Applications*. Plenum Press, New York, 1971.
40. Pyzik, A. J., Deshmukh, U. V., Dummead, S. D., Allen, T. L. and Rossow, H. E., Lightweight boron carbide–aluminum cermets, US Patent No. 5521016, 1996.
41. Chernyshova, T. A. and Rebrov, A. V., Interaction kinetics of boron carbide and silicon carbide with liquid aluminium. *J. Less. Common. Met.*, 1986, **117**, 203–207.
42. Viala, J. C. and Bouix, J., Chemical reactivity of aluminium with boron carbide. *J. Mater. Sci.*, 1997, **32**, 4559–4573.
43. Arslan, G., Kara, F. and Turan, S., Quantitative X-ray diffraction analysis of reactive infiltrated boron carbide–aluminium composites. *J. Eur. Ceram. Soc.*, 2003, **23**, 1243–1255.
44. Fujii, H., Nakae, H. and Okada, K., Interfacial reaction wetting in the boron nitride/molten aluminum system. *Acta Metall. Mater.*, 1993, **41**(10), 2963–2971.
45. Xiao, M. X. and Xiao, F. Y., Spontaneous infiltration of aluminium–silicon alloy into silicon carbide preforms in air. *J. Am. Ceram. Soc.*, 1996, **79**, 102–108.